# EVALUATION AND CORRELATION OF INTER-LABORATORY RESULTS FROM A RAIN EROSION TEST CAMPAIGN

**Edmond F. Tobin*, Trevor M. Young* and Dominik Raps****
***University of Limerick, Limerick, Ireland, **EADS IW, Ottobrunn, Germany**
*edmond.tobin@ul.ie; trevor.young@ul.ie; dominik.raps@eads.net*

**Keywords**: *rain erosion, liquid droplet impact, leading edge coatings*

## Abstract

*An evaluation of six different coatings was completed in a set of inter-laboratory tests, involving three rain erosion test facilities. Results from two whirling arm type test facilities and one water-jet test facility were compared in the test campaign. The surface topography of the test coupons was measured using a confocal laser scanning microscope. Preliminary correlations were concluded between the three test facilities. The incubation period was the main measure of the resistance of the coatings to rain erosion.*

## 1 Introduction

Resistance of aircraft leading edges to high velocity water droplet erosion has, once again, become of keen interest to the aeronautics community. The subject was extensively investigated from the early 1950s to the 1970s, with the main focus of the research directed at supersonic military applications [1-4]. Radomes, in particular, were seen to be vulnerable to this form of erosion [2]. At subsonic speeds, structural materials, such as aircraft-grade aluminium, titanium alloys and steels, provided adequate resistance to the repeated effects of water droplet impact, although paints and other surface finishes could still be damaged. The widespread interest in the use of carbon fibre reinforced composites (CFRP) for commercial aircraft primary structures, including wing and empennage leading edges, has brought the topic to the fore once again. A second driver has come from a renewed interest in laminar flow technologies. Laminar flow can be lost over a section if the roughness of the leading edge increases and causes a laminar–turbulent transition of the boundary layer [5]. Both these drivers come from the constant need to produce more efficient aircraft in terms of weight and fuel consumption. The need to develop new methods for protecting aircraft leading edge from rain erosion follows directly from these emerging trends.

## 2 Inter-laboratory testing

The testing of the resistance of materials and coatings to rain erosion has developed under three main test methods: (1) The whirling arm method incorporates a sample mounted at the end of an arm (Fig. 1 & Fig. 2), which is rotated through an artificial rainfield produced by nozzles or needles [6]; (2) The water-jet method fires a high velocity stream or jet of water onto a stationary test specimen [7,8] (the underlying assumption is that the leading edge of a finite jet will produce a hemisphere-like shape, thus producing a similar damage mechanism as a water droplet); (3) Ballistics/rockets accelerate a sample through an artificial rainfield or to impact a single water droplet [8] (this method is predominantly used for supersonic testing and was not part of the current study).

The objectives of the current study were:

1. To conduct a series of rain erosion tests in three significantly different test facilities – two whirling arm facilities and one water-jet facility;
2. To study the erosion characteristics of six candidate material/coatings (deemed of interest to aircraft leading edges),

where each material/coating is tested under comparable conditions at each of the three facilities; and

3. To compare the erosion damage seen on the test coupons from three test facilities and establish, if possible, a means to correlate results obtained from the different test facilities.

The study is being conducted as part of the European Union (EU) sponsored FP7 project AEROMUCO (AEROdynamic surfaces by advanced MUltifunctional COatings). This project aims to "develop and evaluate a number of alternative – and highly innovative – active and passive multi-functional surface protection systems for future generation of aircraft, leading to a significant improvement in fuel efficiency" [9].

## 3 Description of test rigs

The three test facilities are located at the University of Limerick (UL), Ireland; SAAB, Linköping, Sweden and EADS Innovation Works, Ottobrunn, Germany.

### 3.1 University of Limerick

The Whirling Arm Rain Erosion Rig (WARER) was designed and built at UL. It is based on the principle of a rotating arm with a test coupon mounted at the tip, which is accelerated up to a representative aircraft speed. The WARER was designed to be operated in an open laboratory requiring a compact size. The overall unit including chilling system occupies 5 m$^2$. Water droplets are introduced into the test chamber through 36 blunt dispensing needles with an internal diameter of 0.15 mm. The nominal droplet diameter is 2 mm and the equivalent rainfall rate is 25 mmh$^{-1}$. The droplets fall towards the impact region, protected from the swirling airflow, within a plastic tube or shroud. On exiting the bottom of the shroud, the droplet is impacted by the test coupon. The maximum impact velocity is 178 ms$^{-1}$ which is equivalent to an aircraft operational speed of 300 kt equivalent airspeed at 10,000 ft. The main aspects of the test rig are shown in Fig. 1 (see Tobin *et al.* [6], for further details).

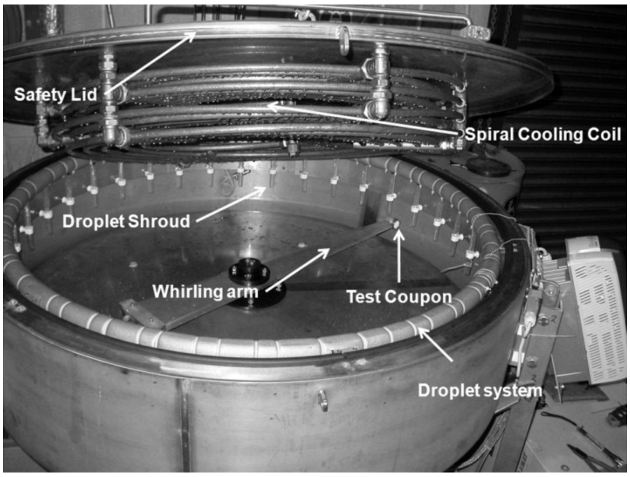


**Fig. 1. WARER at the University of Limerick [6]**

### 3.2 SAAB

The second whirling arm test rig is the SAAB rain erosion test facility. This facility was developed in the 1960s and has a prominent history in the field of rain erosion [10]. The system operates with a test coupon mounted on a rotating arm at a radius of 2.19 m. The system is capable of simulating impact test speeds of up to 300 ms$^{-1}$. The water droplets are produced by six rainfall generators. The droplet size can be varied with nominal diameters of 1.2, 1.6 and 2 mm. The rainfall rate can also be varied from a minimum of 1.4 mmh$^{-1}$ (light drizzle) to a maximum of 25 mmh$^{-1}$ (intense thunderstorm) in 16 steps. An overall view of the testing area can be seen in Fig. 2. The facility has a dedicated test room with an adjacent control room. The facility includes a cctv (closed circuit television) system, which is used to check if the whirling arm is stable at a given test speed. Failure or large amounts of erosion of a test coupon can cause vibration and instability.

**Fig. 2. SAAB rain erosion test facility [11]**

## 3.3 EADS Innovation Works

The third facility is the Pulsating Jet Erosion Test (PJET) facility based at EADS Innovation Works, Ottobrunn. This facility works on the principle of the water jet developed at the Cavendish Laboratories in Cambridge University [8]. A high pressure jet of water is forced through a nozzle of 0.8 mm diameter and is subsequently cut into individual water jets by a rotating disc (Fig. 3). The system is capable of operating at different impact velocities and impact frequencies. The standard test parameters are an impact velocity of 225 ms$^{-1}$ and impact frequency of 40 Hz. The leading edge of the jet produces a curvature approximating that of a 2 mm droplet. This property allows the test method to produce simulated rain erosion conditions.

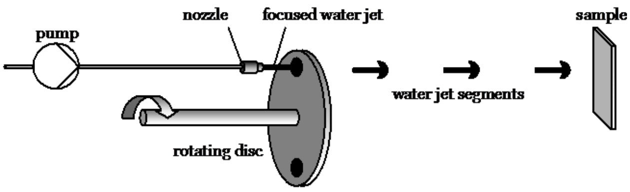


**Fig. 3. Principle of the PJET test method**

# 4 Experimentation

## 4.1 Test parameters

Due to the differences between the test facilities (and the available test schedule), test parameters varied for each facility. However, the simulated rainfall rate, impact angle and droplet size were considered constant.

The test variables at UL were set as follows:

- Impact velocity: 178 ms$^{-1}$,
- Rainfall rate: 25 mm per hour,
- Droplet size: 2 mm diameter (nominal),
- Impact angle: 90°, and
- Test intervals: 2, 5, 10 and 30 minutes.

The test variables at SAAB were set as follows:

- Impact velocity: 180 ms$^{-1}$ and 225 ms$^{-1}$,
- Rainfall rate: 25 mm per hour,
- Droplet size: 2 mm diameter (nominal),
- Impact angle: 90°, and
- Test intervals: until coating failure up to a maximum of 20 minutes.

The test variables at EADS IW were set as follows:

- Impact velocity: 180 ms$^{-1}$ and 225 ms$^{-1}$,
- Rainfall rate: 25 mm per hour,
- Droplet size: 2 mm diameter (nominal),
- Impact angle: 90°, and
- Test intervals: 20, 50, 100, 250, 500, 1000, 2000, 3000 and 6000 impacts.

## 4.2 Materials

The following coatings were tested: a reference material (AA2024 clad aluminium alloy) to calibrate the testing conditions, three current in-service rain erosion resistant coatings and two new experimental coating solutions (Table 1). All coating systems were placed on the same substrate material: AA2024 clad.

**Table 1. Matrix of materials and coatings tested**

| *Materials* | *Type* |
|---|---|
| **AA2024 clad** | Reference |
| **PU topcoat*** | In-Service |
| **PU clearcoat*** | In-Service |
| **PU tape*** | In-Service |
| **Sol-gel (PU silane)** | Experimental |
| **TiN coating** | Experimental |

Note: * indicates commercially available coatings

## 4.3 Evaluation

The test coupons were evaluated after each test interval using three methods: (1) mass loss; (2) surface topography measurements; and (3) appearance (i.e. a qualitative assessment).

## 4.4 Mass loss

Mass loss was recorded for the UL and SAAB tests using analytical balances with an accuracy of 0.1 mg. The coupons were measured before and after testing.

## 4.5 Surface topography

The surface topography was measured using a non-contact method known as Confocal Laser Scanning Microscopy (CLSM). A Zeiss LSM710 CLSM with a 20x EC Epiplan objective was used to measure the topography. The field of view of the objective allows an area 707.4 µm by 707.4 µm to be measured (Fig. 4). This gives an area of approximately 0.5 $mm^2$ over which the surface profile is calculated. Values of the surface topography were produced by the system software. Using a median filter, the arithmetic mean surface area primary profile ($PS_a$) value was produced. The primary profile is the initial profile from which the roughness and waviness profiles are produced. These profiles are produced using the high pass and low pass filters respectively. The average primary profile peak to valley ($PS_z$) was another significant topographical measurement recorded.

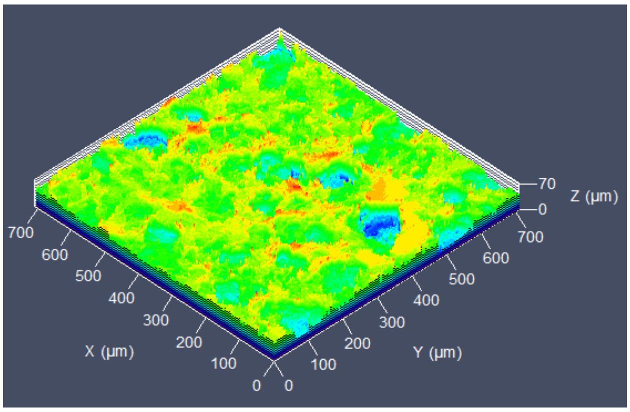


**Fig. 4. Example of a surface area profile produced on AA2024-T3 clad (the red colour indicates peaks and the blue colour indicates valleys).**

## 5 Results

Mass loss and time to coating failure were recorded at the respective test facilities. Test samples were then sent to UL for further analysis. Microscopy and surface topography measurements were completed on all samples.

### 5.1 WARER results

Mass loss results were recorded before and after each test (Fig. 5). Tests of both the topcoat and clearcoat materials did not provide valid mass loss measurements as unexposed edges of the samples were seen to deteriorate. This was due to the method used to cut the circular coupons from the original test panels.

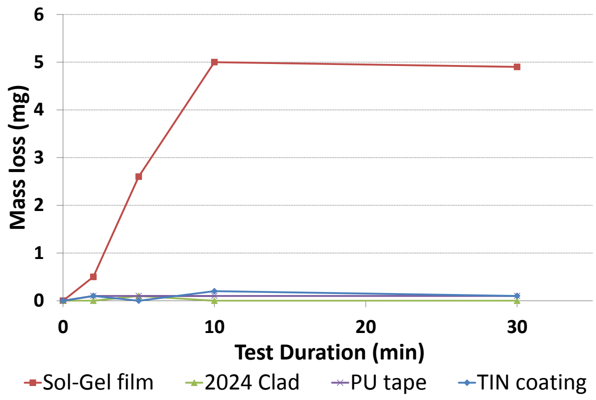


**Fig. 5. Mass loss results from UL tests**

The topography measurements were carried out using the CLSM. The surface was measured at three points along the central region of the test coupon, starting from the top (as mounted) of the coupon. This is due to the fact that the damage begins in this region and then progresses further over the coupon area with increased test duration. The values of interest from the topographical analysis were $PS_a$ and $PS_z$. Results for five of the test sample types are shown in Fig. 6. The Sol-gel results are not presented as the coating was eroded through to the substrate after 2 minutes, meaning that subsequent profile measurements would be invalid.

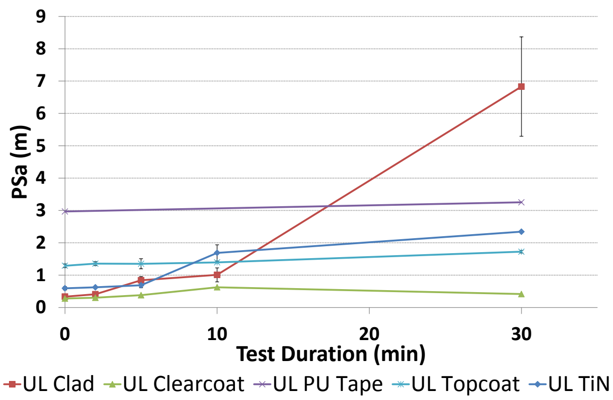


**Fig. 6. $PS_a$ values for tested coatings with standard deviations shown**

The appearance of the coating surface was recorded using a microscope fitted with a digital camera. The progression of erosion with time over the entire test coupon can be seen in the series of images in Fig. 7 for the Sol-gel coated coupons.

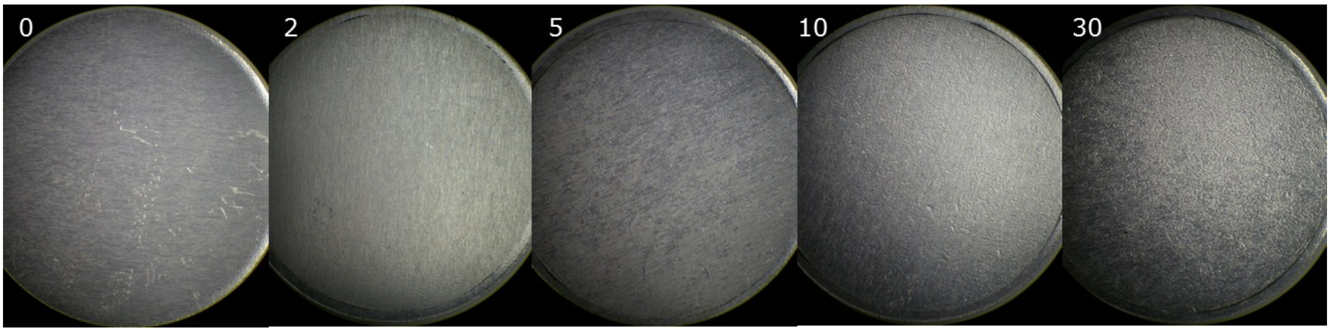


**Fig. 7. Progression of erosion on Sol-gel coated AA2024 sample. The removal of the coating can be seen clearly at 5 minutes, with the substrate damage predominant at 10 and 30 minutes**

## 5.2 SAAB rain erosion test results

The mass of all test coupons was recorded before and after each test. In most cases, this data was a single point recorded at the end of the test after failure of the coupon was recorded. In the case of the three coated test coupons (PU clearcoat, PU topcoat and Sol-gel), this failure was identified by using short duration cumulative tests (1 minute). The PU tape did not fail after 10 minutes of testing at 225 $ms^{-1}$. The TiN coating was tested at 180 $ms^{-1}$ and, although the surface topography changed considerably, there was no significant mass loss recorded (<1 mg). The mass loss of the AA2024 clad coupons was recorded and is presented in Fig. 8. The severity of the 225 $ms^{-1}$ test in comparison to the 180 $ms^{-1}$ test can also be clearly seen in this figure.

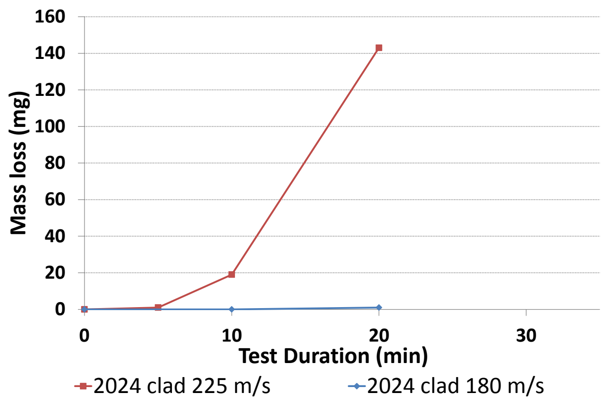


**Fig. 8. Mass of AA2024 clad material tested at SAAB at 180 and 225 $ms^{-1}$**

Topographical measurements were taken of all the test coupons. Five points on the surface of the material/coating were measured. Four measurements were made along the central region of the test coupon, at 10 mm intervals. The final measurement was made at a randomly selected point away from the central region. The Sol-gel results were not considered valid for the reasons mentioned earlier in section 5.1. The test results from both test speeds are presented in Fig. 9.

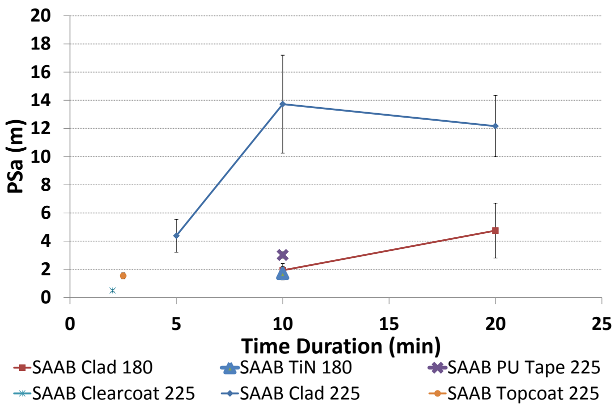


**Fig. 9. Surface area profile values measured from the SAAB tested coupons. The 180 and 225 after each label indicate the test speed in $ms^{-1}$.**

## 5.3 PJET results

The test method of PJET does not allow for the mass loss at each impact number to be measured. Firstly, the impacts are concentrated on a small area of approximately 1 mm in diameter, which is not conducive to removing measureable amounts of material. Secondly, a single test panel is used for all impact numbers meaning that the variation in mass cannot be associated with any particular impact number.

The surface profiles of each impact area were obtained; the averaged values are presented in Fig. 10. The results from both the PU topcoat and the Sol-gel coating were inconclusive. The PU topcoat did not allow for surface profile measurements as the impacts sites were not clearly identifiable. The Sol-gel coating was seen to be removed from the substrate at 50 – 100 impacts. The poor erosive resistance was similarly observed in the results of the whirling arm tests. The PU tape was also tested but the tape failed after 20 impacts. The surface profile was not measure for this reason.

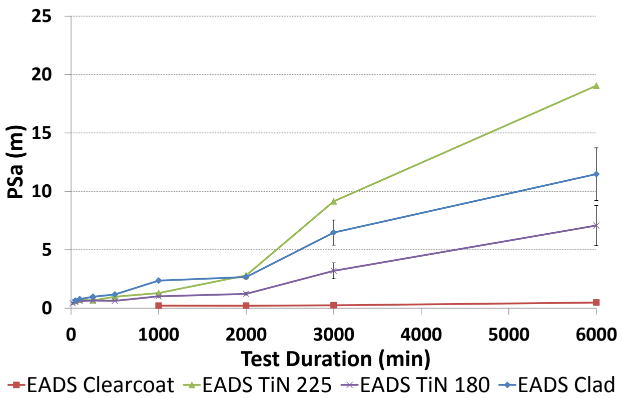


**Fig. 10. Primary profile values from the PJET test rig. Tests were completed at 180 ms$^{-1}$ and 225 ms$^{-1}$ on TiN coating. The other tests were only at 180 ms$^{-1}$.**

## 5.4 Erosion resistance rankings

The results from all tests conducted were compiled and a ranking of the coatings was produced (Table 2). The ranking was based on the incubation period. The incubation period is defined generally as the time taken to erode a test sample sufficiently to record significant mass loss (see Fig. 11 for a graphical explanation). In the case of coatings, and in particular thin coatings, the incubation period can be defined as the time taken to penetrate a coating through to the substrate material. The maximum value of the primary profile of the surface was used as a secondary ranking. The topography of the surface plays an important role in laminar flow and for this reason the surface primary profile is proposed as a separator between materials providing equivalent incubation times.

**Table 2. Ranking of materials tested at 180 ms$^{-1}$**

| *Sample ranking* | *Incubation period* | | | *Max $PS_a$ ($\mu m$)* | | |
|---|---|---|---|---|---|---|
| | UL (min) | SAAB (min) | EADS (impacts) | UL | SAAB | EADS |
| PU tape | > 30 | > 20* | 20 | 3.5 | 3.41* | - |
| PU clearcoat | > 30 | < 2* | > 6000 | 0.62 | 0.63* | 0.48 |
| PU topcoat | < 30 | < 2.5* | > 6000 | 1.78 | 1.83* | 1.34 |
| TiN coating | < 30 | > 10 | < 6000 | 2.37 | 2.57 | 3.2 |
| Sol-gel | < 2 | < 1* | 50 | - | - | - |
| 2024 clad | > 30 | > 20 | < 6000 | 8.14 | 7.41 | 11.48 |

Note: * indicates tests completed at 225 ms$^{-1}$

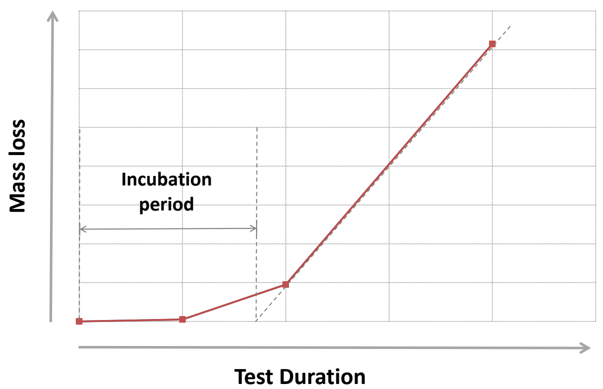


**Fig. 11. Explanation of the incubation period in terms of mass loss**

# 6 Discussion and correlation of test results

Although mass loss results were recorded at a number of test durations for AA2024 clad in both the WARER and SAAB tests, the lack of appreciable mass loss in the WARER tests does not allow a correlation to be established. This is also the case for the SAAB tests at 180 ms$^{-1}$ as a change in mass was only recorded at the longest test duration. This mass loss was also only the minimum amount that was measureable by the scales used.

## 6.1 Correlation of AA2024 clad using the primary surface area profile

Using the surface area primary profile values of the AA2024 clad, a correlation has been attempted for all three tests. The assumption made here is the surface primary profile (roughness and waviness combined) will vary with the erosion conditions seen by the test coupon. The severity of each test will vary and therefore the time/impact number to reach a certain roughness level will also vary.

The $PS_a$ values can be seen to increase with the increase in duration of the test. This increase has been previously shown to be only valid until the incubation period has passed and material removal occurs [6]. After this point, the surface profile values will begin to vary considerably, and in the case of coatings, can begin to reduce as the coating is penetrated through to the substrate material. The correlation of the average $PS_a$ for the WARER and the SAAB rain erosion test (Fig. 12) was found to be 35 minutes (WARER, UL) to 30 minutes (SAAB). Correlation of $PS_z$ also gave a similar relationship (Fig. 13). The average of the primary profile values measured at each data point was used in both correlations. This allowed the average state of the test surface to be compared.

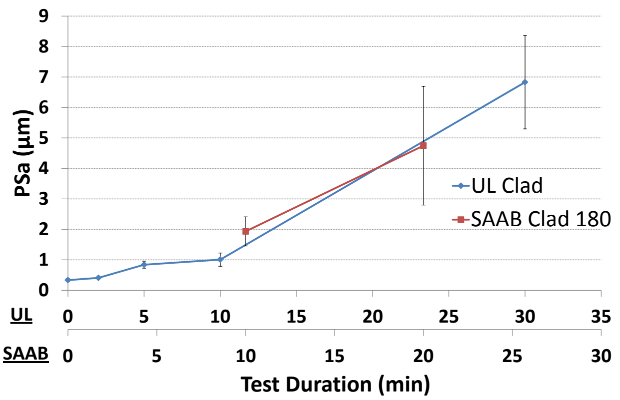


**Fig. 12. Comparison of the surface area profile values versus test duration for both WARER (UL) and SAAB**

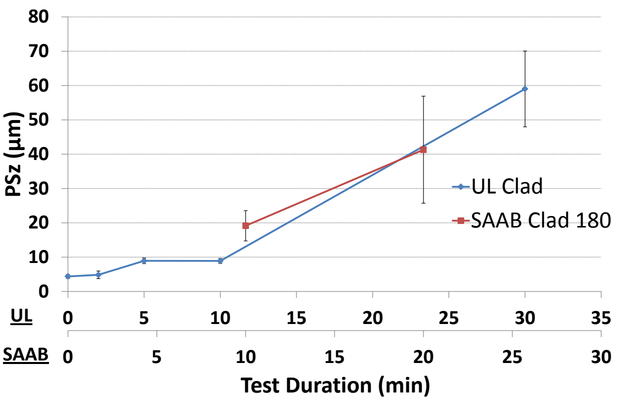


**Fig. 13. Correlation of $PS_z$ for WARER and SAAB results**

A similar approach was used to correlate the PJET results to the WARER AA2024 clad results. As the PJET produces a concentrated point of erosion, the surface topography can be considered to be a maximum value at this point. The WARER distributes impacts over a much larger area with the highest levels of erosion being seen at the top of the coupon as mentioned previously. For this reason, the maximum $PS_a$ and $PS_z$ values, which were taken from the top central region of the coupon, are used for correlation. A correlation of 1000 impacts to 8 minutes was concluded as the best approximation (Fig. 14). The same "exchange rate" or scaling factor was used in Fig. 15 for a correlation of $PS_z$. This is viewed as a preliminary result. It can be seen in both cases that further testing would be required to provide confidence in the scaling values. It should be also noted that the current data differs from results published previously by Tobin *et al.* [6] by approximately a factor of two. $RS_a$ (or $SR_{a)}$, the surface roughness, was previously used which may indicate the reason for the different correlations being established. The waviness of the surface was not taken into consideration in the previous study [6], which can be significant in the highly irregular surfaces produced.

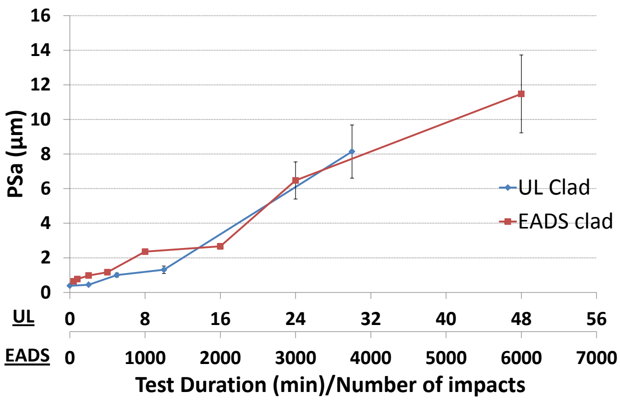


**Fig. 14. Max $PS_a$ values from WARER tests, scaled to correlate with PJET $PS_a$ values**

The final correlation of the PJET results to the SAAB test results are shown in Fig. 16 and Fig. 17. The scaling factor in this correlation was estimated independently from the other correlations. A value of 5.7 minutes to 1000 impacts was calculated. However, when all correlations are compared and cross referenced, it can be seen that the different scaling factors do not correlate to each other. This further indicates that these results can only be considered as preliminary. A further investigation would be required to establish correlations factors to a higher confidence level.

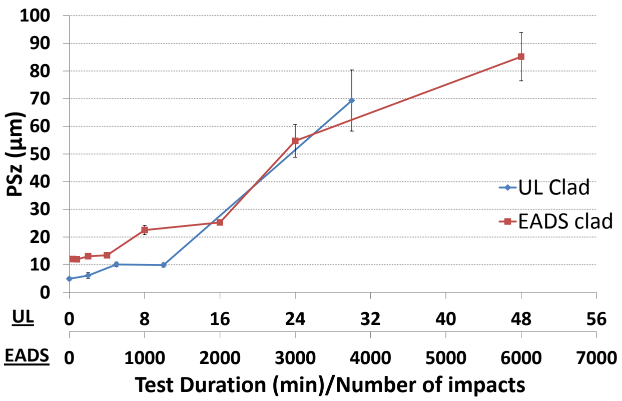


**Fig. 15. Max $PS_z$ from WARER tests and $PS_z$ from PJET tests using the same scaling as Fig. 14**

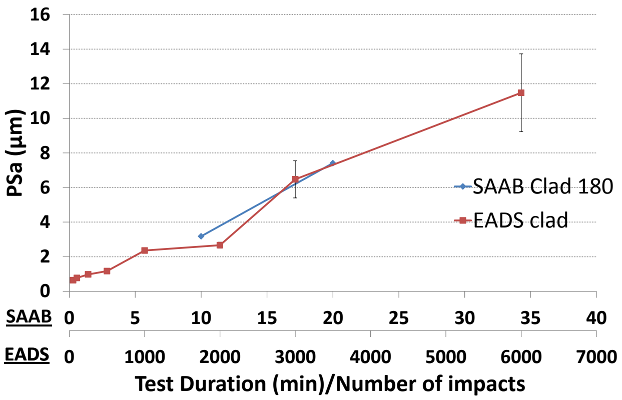


**Fig. 16. Max $PS_a$ from SAAB tests scaled to correlate with PJET $PS_a$ values**

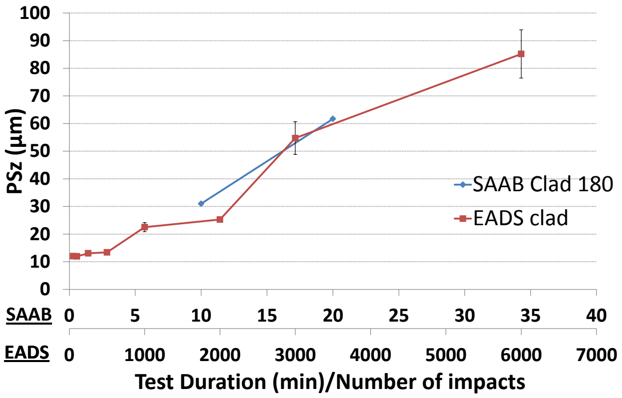


**Fig. 17. Max $PS_z$ from SAAB tests correlated with PJET $PS_z$ values using the same scaling as Fig. 16**

## 6.2 Impact velocity correlation

Following on from the correlations established in section 6.1 based on the surface topography, an attempt was made to correlate the impact velocities from SAAB and EADS. The SAAB test results did show that the $PS_a$ values were much higher from the 225 ms$^{-1}$ tests than the 180 ms$^{-1}$ tests completed on the AA2024 clad coupons. It is important to note that the incubation period had finished and mass removal had begun to occur at the initial (5 minute) test point for the 225 ms$^{-1}$ test. The measurements from the surface are therefore invalid for correlations in this study [6].

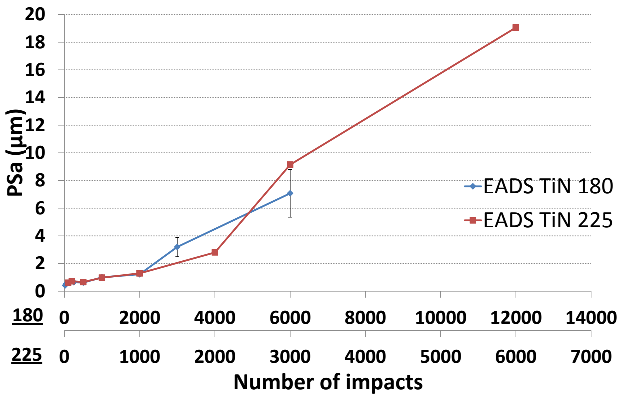


**Fig. 18. Influence of test speed on the number of impacts required to reach a certain primary profile value using the PJET**

The PJET test results included the testing of the TiN coating at 180 ms$^{-1}$ and 225 ms$^{-1}$. The results from this sample showed a considerable amount of surface deformation, due to the thickness of the coating and the soft clad layer of the AA2024 substrate. This allowed a comparison of the surface condition due to the number of impacts and impact velocity. Fig. 18 shows a comparison of the $PS_a$ using a scaling factor of 2 (e.g. 1000 impacts at 180 ms$^{-1}$ are equivalent to 500 impacts are 225 ms$^{-1}$). It can be seen to correlate closely up to 2000 impacts at 180 ms$^{-1}$. The $PS_z$ values for the surface (Fig. 19) are also seen to correlate closely to the same point. The subsequent divergence can be explained as an indication of the ending of the incubation period at approximately 3000 or 1500 impacts, respectively. This would be in line with the indications given from the correlations with the WARER and SAAB test results. Both the WARER and SAAB test showed indications of mass loss at test durations equivalent 3000 impacts at 180 ms$^{-1}$ on the AA2024 clad and TiN coating test coupons. This correlation is solely based on the TiN experimental results and may not be valid for other materials or coating.

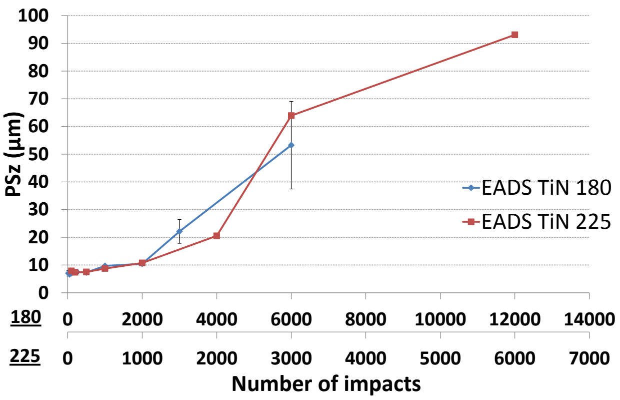


**Fig. 19. Correlation of the tests speeds of the PJET using $PS_z$ values**

## 6.3 Factors affecting correlation of results

Some of the factors that affect the correlation of inter-laboratory testing of materials for rain erosion resistance, which were not noted previously, are discussed in this section.

### *6.3.1 Test coupon size*

The size of the test coupon is important when correlating results. In this study, the circular coupons used by UL and SAAB had an exposed diameter of 25 mm and 44 mm, respectively. In order to correlate mass loss results, the exposed surface area needs to be calculated. The SAAB test coupon has a surface area three times larger than that of the WARER test rig. This would mean under ideal test conditions with uniformly distributed impacts and equal test speeds that a test coupon of 44 mm diameter should see a mass loss approximately three times higher than that of a 25 mm diameter test coupon for the same test duration.

### *6.3.2 Droplet distribution*

A factor leading on from the coupon size and uniform mass loss over a test coupon is droplet distribution. The PJET method is based on the principle of concentrating the jets (equivalent droplets) to accelerate the erosion of the test material. The SAAB test rig and the WARER are based on the principle of distributed droplet impacts. The test results from SAAB show that there is a general distribution of droplets over the whole exposed surface of the test coupon. However, bands of erosion can be seen on closer inspection, indicating a concentration of droplets which may be caused by the manner in which the rainfield is generated. In respect of the WARER, the conditions are different again. It can be clearly seen that the impacts tend to cluster to the top of the coupon [12], leading to erosion initiating in this area and progressively spreading over the coupon. The progression of damage/erosion over the coupon is seen to also vary with impact velocity.

### *6.3.3 Droplet impact intensity*

A variation in the distribution of impacts may cause higher impact frequencies and intensities. In the case of the WARER, this may be account of the spreading of the damage/erosion over the coupon. It can also provide some anomalies in the tests results, as can be seen by the failure of the PU tape at low impact numbers when tested in the PJET while no failure was recorded in either the WARER or the SAAB test rig up to 30 minutes test duration. It has been shown, in other tests of elastomeric coatings, that the intensity seen in the PJET is strongly linked to the test velocity. Previous tests of PU tape at 140 $ms^{-1}$ have shown no erosion effects (results not included in this paper).

## 7 Conclusions

The inter-laboratory testing of a variety of coatings provided interesting results that permitted a preliminary correlation between three significantly different rain erosion test facilities to be established. The use of surface topographical measurements (i.e. $PS_a$ and $PS_z$) using a CLSM proved successful for the comparison of test results. The surface morphology was seen to change with increasing test duration in all three test facilities providing a measure of the level of erosion on most of the materials. The PU topcoat and PU tape performed differently under the PJET test conditions compared to the whirling arms conditions for the WARER and the SAAB test rig.

## Acknowledgements

This research is supported by the European Union through FP7 Framework project AEROMUCO (AEROdynamic surfaces by advanced MUltifunctional COatings). The authors would like to acknowledge the following people for their collaboration in the inter-laboratory test campaign: Oliver Rohr at EADS IW, Ottobrunn, Germany; Wim Willemse and Peter Norman at SAAB, Linköping, Sweden. The authors would also like to acknowledge the following organisations for providing test materials and data for this study: HEF R&D, Andrezieux-Boutheon, France; Dassault Aviation SA, Paris, France and CREST, Dublin Institute of Technology, Dublin, Ireland.

## References

[1] Busch H, Hoff G, Langbein G. A Discussion on Deformation of Solids by the Impact of Liquids, and its Relation to Rain Damage in Aircraft and Missiles, to Blade Erosion in Steam Turbines, and to Cavitation Erosion. *Philosophical Transactions of the Royal Society, Series A, Mathematical and Physical Sciences*, Vol. 260, No. 1110, pp 168-181, 1966.

[2] Fyall AA. Practical aspects of rain erosion of aircraft and missiles, A Discussion on Deformation of Solids by the Impact of Liquids, and its Relation to Rain Damage in Aircraft and Missiles, to Blade Erosion in Steam Turbines, and to Cavitation Erosion. *Philosophical Transactions of the Royal Society. Series A, Mathematical and Physical Sciences*, Vol. 260, No. 1110, pp 161-167, 1966.

[3] Methven TJ, Fairhead B. A Correlation between Rain Erosion of Perspex Specimens in Flight and on a Ground Rig. ARC-TR-21-090. 1960.

[4] Schmitt GF and Hurley CJ. Development and calibration of a Mach 1.2 rain erosion test apparatus. AFML-TR-70-240, Air Force Materials Laboratory, Wright-Patterson Air Force Base, Ohio, 1970.

[5] Young TM, Humpherys B. Fielding JP. Investigation of hybrid laminar flow control (HLFC) surfaces. *Aircraft Design*, 4, pp. 127-146, 2001.

[6] Tobin EF, Young TM, Raps D and Rohr O. Comparison of liquid impingement results from whirling arm and water-jet rain erosion test facilities. *Wear,* 271, pp. 2625-2631, 2011.

[7] Alder WF. Rain impact retrospective and vision for the future. *Wear*, 233-235, pp. 25-38, 1999.

[8] Obara T, Bourne NK and Field JE. Liquid-jet impact on liquid and solid surfaces. *Wear*, 186-187, pp. 388-394, 1995.

[9] Project AEROMUCO, www.aeromuco.eu/ [Last accessed 10 July 2012]

[10] Eskilsson S. Rain erosion testing facilities at Saab and some test results. *Proceeding of the Rain Erosion Conference,* Meersburg, Germany, 3.5, pp 43-48, 1965.

[11] SAAB Group website, www.saabgroup.com/en/commercial-aeronautics/engineering-services/ testing/environmental-testing/ [Last accessed 10 July 2012]

[12] Tobin EF, and Young TM. Characterisation tests of a whirling arm rain erosion test facility using aluminium alloy. *5th International Supply on the Wings Conference,* Frankfurt, 2010.